06

Investigation of non-uniformity of properties of niobium nitride thin films obtained by atomic layer deposition

© M.V. Shibalov,[1] A.A. Shibalov,[1] A.R. Shevchenko,[1] A.M. Mumlyakov,[1] I.A. Filippov,[1] M.A. Tarkhov[1,2]

[1] Institute of Nanotechnology of Microelectronics, Russian Academy of Sciences,
119991 Moscow, Russia
[2] National Research University „Moscow Power Engineering Institute“,
111250 Moscow, Russia
e-mail: maxshibalov@gmail.com

Received May 17, 2024
Revised September 24, 2024
Accepted October 6, 2024

In this work we studied the non-uniformity of properties of niobium nitride thin film obtained by atomic layer deposition enhanced by plasma on 100 mm silicon substrate with a layer of silicon oxide. The non-uniformity of the surface resistivity distribution was 7% at a diameter of 92 mm. The film thickness distribution non-uniformity measured by X-ray reflectometry at the central part of the wafer and at 4 locations 40 mm away from the centre was 4%. X-ray diffraction performed at the same locations on the wafer showed no visible reflex shifts. The variation in the lattice parameter for the different regions was only 0.06%. Superconducting measurements showed a maximum deviation of 1.6% for the superconducting transition temperature and 7% for the critical current density at a diameter of 80 mm.

Keywords: atomic layer deposition, plasma, niobuim nitride, non-uniformity, critical temperature, critical current density.

DOI: 10.61011/TP.2025.01.60510.183-24

Introduction

The interest in the production and study of thin films of niobium nitride (NbN) obtained by plasma-enhanced atomic layer deposition (PEALD) has significantly increased recently [1–3]. This method makes it possible to meet the needs for atomic control of the film growth rate, conformal and homogeneous deposition owing to the use of sequential, self-limited chemical surface reactions [4,5]. If each of the two surface reactions is self-limited, then these two reactions can proceed sequentially, ensuring thin film deposition with control at the atomic level. The obtained films are usually solid and do not have holes since there should be no unoccupied surface areas on the substrate surface during the film growth. This factor is extremely important for the deposition of high-quality films on technological substrates. Two reactants in the gas phase also do not contact with each other because the surface reactions proceed separately. This separation of the two reactions limits the possible side effects of gas-phase reactions, which can result in the formation of particles capable of settling on the surface of the substrate and creating rough films with inclusions of particles.

NbN thin films are used in various superconducting devices and passive elements, such as hot electron bolometers (HEB) [6], superconducting tunnel junction detectors (STJ) [7], parametric amplifiers (TWPA) [8], single-photon detectors (SNSPD) [9,10], superconducting delay lines [11]. NbN films with high uniformity of thickness and characteristics are required for the scalable manufacturing of such devices . For example, the total length of a TWPA can reach several centimeters, since the amount of gain depends on the total length. Insufficient uniformity of the NbN film can result in the deterioration of the parameters of these amplifiers. The uniformity of the characteristics of NbN superconducting thin films becomes an important parameter with the transition from single-pixel to multi-pixel SNSPD-based devices, which are needed, in particular, for visualization applications [12,13]. The temperature of the transition to the superconducting state and the critical current density of each detector in a multi-pixel device should have a minimum deviation from each other. That is why PEALD NbN is of great interest to many researchers. Films with a thickness heterogeneity of less than 1% on a 100 mm substrate can be obtained using the thermal method of atomic layer deposition. However, the uniformity of the PEALD metal nitride process for chlorine-free precursors has not been sufficiently studied unlike the ALD thermal process, the uniformity of which has been well studied with respect to dielectric films of metal oxides and some conductive films of metal nitrides [14–16] obtained from chloride precursors. The authors of Ref. [17] achieved a heterogeneity of the temperature of transition to the superconducting state and the critical current density equal to 1 and 12%, respectively, over a diameter of 2 inches. The researchers obtained a heterogeneity of the temperature of transition to the superconducting state and the critical current density equal to 4.5 and 39%, respectively, over a diameter of 4 inches on a monocrystalline silicon substrate

in Ref. [18]. There is a heterogeneity associated with the plasma distribution in the PEALD processes, in addition to the sources of heterogeneity that are present in the ALD thermal process, such as overlapping of the material supply pulses, uneven distribution of the precursor in the carrier gas, temperature heterogeneity on the substrate surface, etc. [16]. The parameters of the plasma pulse can change the quantity and quality of the reaction elements in the gas phase above the substrate, as well as the reaction sites on the substrate. Thus, a uniform plasma density is crucial for obtaining a good film uniformity. We study in this paper an NbN thin film obtained by the PEALD method on a silicon substrate with an amorphous silicon oxide layer. We use a silicon substrate with amorphous silicon oxide and study the heterogeneity of surface resistance, thickness, crystal lattice parameter, superconducting transition temperature and critical current density compared to Ref. [18], where NbN film was grown on a single-crystal silicon substrate. The study of the heterogeneity characteristics of an NbN film on an amorphous silicon oxide sublayer will further make it possible to produce an NbN film with the required heterogeneity parameters on a distributed Bragg reflector or waveguides made of amorphous silicon nitride.

1. Experiment

A silicon substrate of *n*-type with a diameter of 4 inches was chosen as the substrate for deposition. The substrate was washed in a hydromechanical washing unit before deposition of the layers. The substrate was loaded into the airlock chamber after washing and was transferred to the plasma chemical deposition chamber to form SiO_2 film with a thickness of 100 nm. The substrate was transferred to the atomic layer deposition chamber without breaking the vacuum cycle after the deposition of SiO_2 film. The NbN film was deposited by repeating the reaction series, including feeding of the organometallic precursor TBTDEN (tris(diethylamido)(tert-butylimido) niobium(V)) and two reactants consisting of two different gas mixtures. The first reactant was NH_3/Ar gas mixture. The second reactant was immediately supplied after the exposure to the plasma of the first reactant and the plasma was ignited. H_2/Ar gas mixture was used as the second reactant. The NbN atomic layer deposition process consisted of five main stages. The organometallic precursor TBTDEN (3 s, 55 mTorr) was supplied at the first stage. The chamber was purged with argon (5 s, 50 mTorr) after exposure to the precursor. The first reactant, NH_3/Ar gas mixture, was supplied next, and plasma was ignited. The second reactant, H_2/Ar gas mixture, was supplied after the exposure to the plasma of NH_3/Ar gas mixture, and the plasma was also ignited. The chamber was purged with argon (10 s, 100 mTorr) at the end of the cycle to remove the reaction products. 96 deposition cycles were used. Deposition was performed at a temperature of 350°C. The pressure in the chamber at the plasma exposure stage was determined by the ratio of fluxes of NH_3/Ar and H_2/Ar gases with the flap fully open and was in the range of 3–4 mTorr. The power of the inductively coupled plasma (ICP) source was 100 W.

The surface resistance of the NbN film was measured by a four-probe method using 4D Automatic Four Point Probe Meter Model 280 probe station that can build a distribution map over the surface of a 100 mm plate. The diameter of the substrate for plotting the surface resistance map was 92 mm to avoid measurements at the edges of the plate. The surface resistance distribution map was measured at 25 points.

The thickness of the studied samples was determined by X-ray reflectometry. The reflectograms were acquired using an X-ray diffractometer, in the geometry of a parallel mirror and a parallel-plate collimator, using a proportional detector. Reflectogram scanning mode: ω-2θ using radiation CuK_α ($\lambda = 1.540605$ Å), with an accelerating voltage of 45 kV and 40 mA. Scanning step 0.003, exposure 2 s. The specialized software AMASS was used for the analysis and processing of the obtained reflectograms.

Grazing incidence X-ray diffraction (GIXRD) was performed to study the crystal structure and determine the crystal lattice parameters of NbN thin films. An X-ray diffractometer with a proportional detector was used for the study. The diffraction patterns were taken in the angle scanning mode 2θ at the angle of incidence of X-ray radiation on the sample $\omega = 0.5°$ using radiation CuK_α ($\lambda = 1.540605$ Å) with an accelerating voltage of 45 kV and 40 mA. The scanning step was 0.05°, and the exposure was 2 s. The diffraction patterns were processed and analyzed using specialized software HighScore.

The critical temperature of the transition to the superconducting state and the magnitude of the critical current were measured in a Gifford–McMahon closed-loop cryostat, cooled to a temperature of 2.4 K. The sample was thermally conditioned using a cryogenic holder with an integrated and calibrated thermometer and a resistive heater. PID-controller was used for automatic thermometry and temperature control.

Micro bridges with a width of 2 μm were formed on niobium nitride films using contact lithography to measure the critical current. Niobium nitride was etched in a reactor with ICP-plasma in a mixture of SF_6/Ar gases (gas flux ratio 2 : 1). The width of the formed micro bridges was controlled using optical and scanning electron microscopes for precise control of the critical current density. The critical current was measured using a two-point measurement scheme with low-noise precision current source Keithley 6221A. The dependence of the critical current density on temperature was studied using the current-voltage curve obtained in the voltage stabilization mode at a fixed temperature. The critical current density was determined based on the magnitude of the critical current and the geometric dimensions of the studied sample.

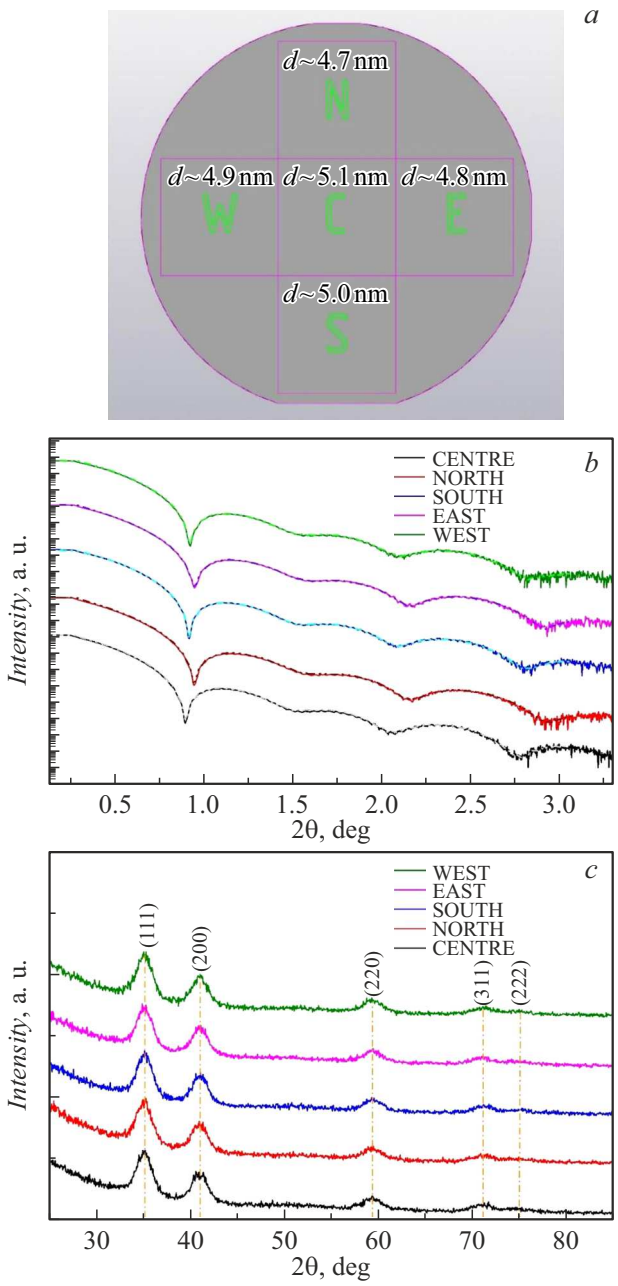

Figure 1. Schematic representation of the substrate with XRR, GIXRD zones (*a*). The measured NbN film thickness is indicated on each zone. Reflectograms for different zones on a substrate (*b*). Diffraction patterns for different zones on a substrate (*with*).

2. Results and discussion

A plate with NbN film was placed on the goniometer table for recording reflectograms and diffraction patterns. When X-ray reflectometry (XRR) and GIXRD are performed, the study is conducted at grazing angles of inclination of the X-ray source, therefore, the X-ray spot on the sample has an elongated shape and is limited by a system of masks and slits of the focusing system. Fig. 1, *a* schematically shows the examined zones for XRR- and GIXRD-analysis. The central area of the substrate was initially scanned, then the substrate was shifted relative to the center by 40 mm along the directions X and Y, after which the scanning was also conducted. NbN film thicknesses were determined in various zones of the substrate after processing the received reflectograms shown in Fig. 1, *b* and the results are listed in Table 1. The difference of the positions and frequencies of the resonances on the reflectograms indicates a different thickness of the deposited film. The position difference may also depend on the superposition of different layers of the sample, for example, an NbN film and a top layer of niobium oxide oxidized by atmospheric oxygen. However, no oxidized layer was observed since the reflectograms were recorded immediately after deposition of the niobium nitride film. An inert transfer medium was not used. The heterogeneity of the film thickness distribution, calculated using the formula: $U_d = (d_{\max} - d_{\min})/2 \cdot d_{mean}$, where $d_{\max}$, $d_{\min}$ is the maximum and minimum measured NbN film thickness, d_{mean} is the average thickness of NbN film that was 4% over a diameter of 80 mm. It can also be noted that there is some thickening in the central part of the substrate relative to the lateral parts. Fig. 1, *c* shows diffraction peaks recorded in different areas of the substrate. The analysis of the obtained diffraction patterns shows that the film in all parts of the substrate consists of δ-phase Nb_xN_y with cubic syngony. The chemical composition of the film has not been studied in this paper. However, a special two-stage deposition procedure with two nonmetallic reagents NH_3/Ar and H_2/Ar was used to reduce the amount of carbon in the growing film from the organometallic precursor and residual oxygen in the process chamber. The carbon is effectively removed at the NH_3/Ar plasma exposure step, and the growing NbN film is reduced at H_2/Ar plasma exposure stage. It should also be noted that the study of the chemical composition of a film with a thickness of less than 5 nm by Auger electron spectroscopy is complicated because of the strong mixing during sputtering by an argon beam. The crystal lattice parameter of δ-phase was calculated for each diffraction pattern based on reflections (200), (220) and (311) and on average it is equal to 4.40 Åfor all studied regions. The heterogeneity of the lattice parameter was only 0.07%. The calculated values of the lattice parameter are shown in Table 1. It is worth noting that when the substrate is shifted relative to the central point by 40 mm in all directions, the diffraction peaks do not shift and their intensity does not change.

The temperature dependences of the resistance of micro bridges for samples from different parts of the substrate are shown in Fig. 2. The heterogeneity of the temperature of transition to the superconducting state was 1.6%. There is no obvious dependence of the transition temperature on the location of the sample on the substrate according to the dependences obtained.

The surface resistance map for NbN film is shown in the lower part of Fig. 3. The average value of the surface resistance was 375 Ω/sq. The heterogeneity of the surface

Table 1. Calculated film thicknesses and crystal lattice parameter for NbN film depending on location on substrate

Scanning area	Film thickness, nm	Lattice parameter, Å
Centre	5.1 ± 0.3	4.404
South	5 ± 0.3	4.398
North	4.7 ± 0.3	4.404
West	4.9 ± 0.3	4.401
East	4.8 ± 0.3	4.404

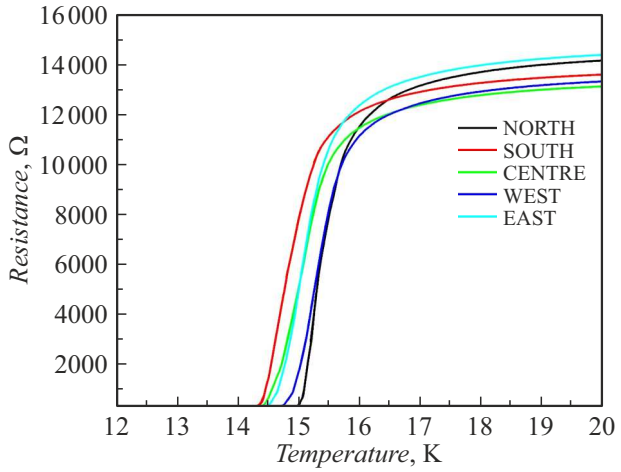

Figure 2. Temperature dependences of the resistance depending on the location of the samples on the substrate.

resistance distribution is 7.5% over a diameter of 92 mm. It is clearly visible on the map that a zone in the central part of the substrate has a lower surface resistance than the area along the edges of the substrate. 9 samples with fabricated micro bridges were measured to determine the heterogeneity of the critical current density. 4 samples on each side of the substrate at a distance of 25 mm from the center, 4 samples at a distance of 40 mm from the center, and a sample located in the central part were used for this purpose. The distribution of the critical current density is shown in the upper part of Fig. 3. It can be seen that the critical current density in the center of the substrate has the highest value equal to 4.6 MA/cm^2. As we move away from the center of the substrate, the critical current density decreases in both directions to 4 MA/cm^2. For comparison, Table 2 shows the values of the critical current density for films obtained by various methods.

As can be seen from the table, the atomic layer deposition method is not inferior in terms of critical current density to the magnetron sputtering method.

The heterogeneity of the critical current density was 7% over a diameter of 80 mm. This distribution of surface resistance and critical current density is directly related to the configuration of the setup, the diameter of the inductively coupled plasma source, and the selected operating pressure. The plasma source is located at a distance from the substrate in the atomic layer deposition with a remote plasma source, which is used in this study. Thus, the substrate is practically not involved in plasma generation. However, unlike atomic layer deposition with radical enhancement, plasma is still present above the substrate surface, and electron and ion densities have a nonzero value. The plasma in the „downstream“ region, i.e. directly under the source bulb, can be active enough to ionize the substrate surface. The increased free path of electrons and ions due to the low pressure operation is combined with the effect of directed ion bombardment in the central part of the substrate because of which there are differences in the characteristics of the film. It has been shown in a number of studies that the lower the pressure at the step of exposure to the nonmetallic reactant plasma during the growth of the NbN film, the higher the superconducting characteristics and the lower the resistivity of the film. Low pressure operation is a crucial factor for producing high-quality NbN films. The uniformity of films can be improved in two ways based on this. It is the use of a plasma source with a larger diameter or the use of a second

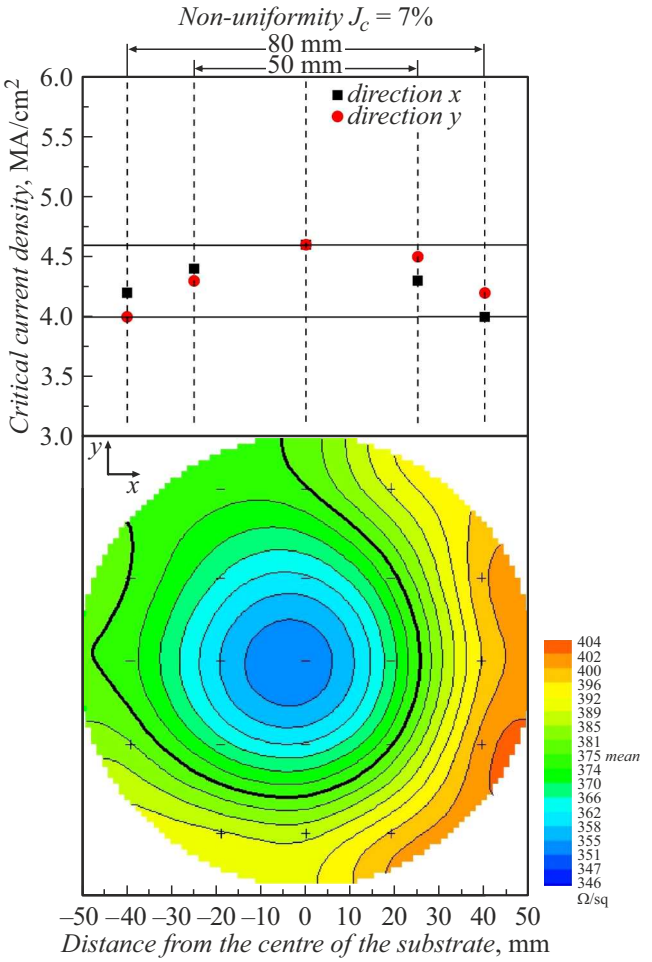

Figure 3. The distribution of the critical current density and the surface resistance map on the diameter of 50 and 80mm, respectively.

Table 2. Values of the critical current density and its heterogeneity for films obtained by various methods

Authors	Obtaining method	Substrate	T_{sub}, °C	d, nm	T_c, K	J_c, MA/cm^2	Deviation J_c of diameter 2 inches, %
D. Dochev et al. [19]	Magnetron sputtering	SiO_2	800	≈ 8.6	9.3	1.14	–
R. Romestain et al. [20]	Magnetron sputtering	Al_2O_3	600	6.4	11.3	4.6	–
R. Espiau de Lamaëstre et al. [21]	Magnetron sputtering	Al_2O_3	600	4.4	11.3	4	–
M. Ziegler et al. [22]	Atomic layer deposition	SiO_2	350	28	14	7.1	–
S. Linzen et al. [23]	Atomic layer deposition	SiO_2	350	40	13.8	7	–
E. Knehr et al. [17]	Atomic layer deposition	SiO_2	380	6.1	10.3	5.7	12
M. Shibalov et al. [1]	Atomic layer deposition	SiO_2	350	7	12.3	9	–
This paper	Atomic layer deposition	SiO_2	350	4.9	15	4.6	1

source, due to which an external bias can be applied to actively bombard the substrate surface at a higher pressure.

Conclusion

The atomic layer deposition method ensures high uniformity of films, especially for the processes of thermal deposition of transition metal oxides. However, the uniformity of the films produced by the atomic layer deposition enhanced by metal nitride plasma strongly depends on the reactor configuration and deposition process parameters. This is associated with the heterogeneity of the plasma distribution in the process chamber.

The heterogeneity of the characteristics of the NbN film obtained by the PEALD method on a 100 mm substrate at various points was studied in the paper. We have achieved a surface resistance heterogeneity of 7.5% over a diameter of 92 mm and 3% over a diameter of 50 mm. The heterogeneity of the film thickness and the lattice parameter was 4 and 0.06

Funding

The study was supported by the project № 122040800157-8 of the Ministry of Education and Science of the Russian Federation. The study was conducted using equipment from the LSRF „ECHIT“ of Institute of Nanotechnology Microelectronics of the Russian Academy of Sciences.

Conflict of interest

The authors declare that they have no conflict of interest.

References

[1] M.V. Shibalov, A.M. Mumlyakov, I.V. Trofimov, E.R. Timofeeva, A.P. Sirotina, E.A. Pershina, A.M. Tagachenkov, Y.V. Anufriev, E.V. Zenova, M.A. Tarkhov. Superconductor Science Technol., **34** (8), 085016 (2021). DOI: 10.1088/1361-6668/ac0d09

[2] M.V. Shibalov, A.P. Sirotina, E.A. Pershina, V.P. Martovitskii, A.A. Shibalova, A.M. Mumlyakov, I.V. Trofimov, E.R. Timofeeva, N.V. Porokhov, E.V. Zenova, M.A. Tarkhov. Appl. Surf. Sci., **612**, 155697 (2023). DOI: 10.1016/j.apsusc.2022.155697

[3] M.J. Sowa, Y. Yemane, J. Zhang, J.C. Palmstrom, L. Ju, N.C. Strandwitz, B.P. Fritz, J. Provine. J. Vacuum Sci. Technol. A, **35** (1), (2017). DOI: 10.1116/1.4972858

[4] S.M. George. Chem. Rev., **110** (1), 111 (2010). DOI: 10.1021/cr900056b

[5] M. Ritala, M. Leskelä. Handbook of Thin Films (2002). DOI: 10.1016/B978-012512908-4/50005-9

[6] S.A. Ryabchun, I.V. Tretyakov, M.I. Finkel, S.N. Maslennikov, N.S. Kaurova, V.A. Seleznev, B.M. Voronov, G.N. Goltsman. Signal, **270**, 320 (2008).

[7] L. Parlato, G. Peluso, G. Pepe, U.S. di Uccio, R. Cristiano, E. Espositio, L. Frunzio, S. Pagano, H. Akoh, H. Nakagawa, S. Takada, M. Gutsche, H. Kraus. Nuclear Instruments and Methods in Physics Research Section A: Accelerators, Spectrometers, Detectors and Associated Equipment, **370** (1), 95 (1996). DOI: 10.1016/0168-9002(95)01060-2

[8] B.K. Tan, F. Boussaha, C. Chaumont, J. Longden, J.N. Montilla. Open Research Europe, **2**, (2022).
[9] G.N. Gol'Tsman, O. Okunev, G. Chulkova, A. Lipatov, A. Semenov, K. Smirnov, B. Voronov, A. Dzardanov, C. Williams, R. Sobolewski. Appl. Phys. Lett., **79** (6), 705 (2001). DOI: 10.1063/1.1388868
[10] F. Marsili, F. Najafi, E. Dauler, F. Bellei, X. Hu, M. Csete, R.J. Molnar, K.K. Berggren. Nano Lett., **11** (5), 2048 (2011). DOI: 10.1021/nl2005143
[11] G.K.G. Hohenwarter, E.K. Track, R.E. Drake, R. Patt. IEEE Transactions Appl. Superconductivity, **3** (1), 2804 (1993). DOI: 10.1109/77.233499
[12] Y.Z. Wang, W.J. Zhang, X.Y. Zhang, G.Z. Xu, J.M. Xiong, Z.G. Chen, Y. Hong, X. Liu, P. Yuan, L. Wu, Z. Wang, L.X. You. arXiv preprint arXiv:2402.02311. (2024).
[13] G.G. Taylor, D. Morozov, N.R. Gemmell, K. Erotokritou, S. Miki, H. Terai, R.H. Hadfield. Opt. Express, **27** (26), 38147 (2019). DOI: 10.1364/OE.27.038147
[14] D. Koushik, M. Jošt, A. Dučinskas, C. Burgess, V. Zardetto, C. Weijtens, M.A. Verheijen, W.M.M. Kessels, S. Albrecht, M. Creatore. J. Mater. Chem. C, **7** (40), 12532 (2019). DOI: 10.1039/C9TC04282B
[15] J.A. Oke, T.C. Jen. J. Mater. Res. Technol., (2022). DOI: 10.1016/j.jmrt.2022.10.064
[16] K.E. Elers, T. Blomberg, M. Peussa, B. Aitchison, S. Haukka, S. Marcus. Chem. Vapor Deposition, **12** (1), 13 (2006). DOI: 10.1002/cvde.200500024
[17] E. Knehr, M. Ziegler, S. Linzen, K. Ilin, P. Schanz, J. Plentz, M. Diegel, H. Schmidt, E. Il'ichev, M. Siegel. J. Vacuum Sci. Technol. A, **39** (5), (2021). DOI: 10.1116/6.0001126
[18] C.T. Lennon, Y. Shu, J.C. Brennan, D.K. Namburi, V. Varghese, D.T. Hemakumara, L.A. Longcha, S. Srinath, R.H. Hadfield. Mater. Quant. Technol., **3** (4), 045401 (2023). DOI: 10.1088/2633-4356/ad0aa5
[19] D. Dochev, V. Desmaris, A. Pavolotsky, D. Meledin, Z. Lai, A. Henry, E. Janzén, E. Pippel, J. Woltersdorf, V. Belitsky. Superconductor Sci. Technol., **24** (3), 035016 (2011). DOI: 10.1088/0953-2048/24/3/035016
[20] R. Romestain, B. Delaet, P. Renaud-Goud, I. Wang, C. Jorel, J.C. Villegier, J.P. Poizat. New J. Phys., **6** (1), 129 (2004). DOI: 10.1088/1742-6596/97/1/012087
[21] R. Espiau de Lamaëstre, P. Odier, J.C. Villégier. Appl. Phys. Lett., **91** (23), (2007). DOI: 10.1063/1.2820607
[22] M. Ziegler, S. Linzen, S. Goerke, U. Brückner, J. Plentz, J. Dellith, A. Himmerlich, M. Himmerlich, U. Hübner, S. Krischok, H.G. Meyer. IEEE Transactions Appl. Superconductivity, **27** (7), 1 (2017). DOI: 10.1109/TASC.2017.2744326
[23] S. Linzen, M. Ziegler, O.V. Astafiev, M. Schmelz, U. Hübner, M. Diegel, E. Il'ichev, H.G. Meyer. Supercond. Sci. Technol., **30** (3), 035010 (2017). DOI: 10.1088/1361-6668/aa572a

Translated by A.Akhtayamov